Left-handed metamaterials with saturable nonlinearity

A. Maluckov,[1] Lj. Hadžievski,[2] N. Lazarides,[3,4] and G. P. Tsironis[3]
[1]*Faculty of Sciences and Mathematics, Department of Physics, P.O. Box 224, 18001 Niš, Serbia*
[2]*Vinča Institute of Nuclear Sciences, P.O. Box 522, 11001 Belgrade, Serbia*
[3]*Department of Physics, University of Crete, and Institute of Electronic Structure and Laser, Foundation for Research and Technology–Hellas, P.O. Box 2208, 71003 Heraklion, Greece*
[4]*Department of Electrical Engineering, Technological Educational Institute of Crete, P.O. Box 140, Stavromenos, 71500 Heraklion, Crete, Greece*
(Received 21 November 2007; published 21 April 2008)

The left-handed properties of metamaterials with saturable nonlinearity are analyzed with respect to their electromagnetic response as a function of externally varying parameters. We demonstrate that the response of the medium is strongly affected by the saturation of the nonlinear effects. The last can be exploited to modulate the amplitude or tune the frequency of the response. Moreover, the existence of bistability regions in large parts of the external parameter space allows for switching between different magnetization states, with either positive or negative response. The stability issue of multiple possible states is addressed through modulational instability analysis of plane wave envelopes in each of those states.

DOI: 10.1103/PhysRevE.77.046607 PACS number(s): 41.20.Jb, 78.20.Ci, 42.25.Bs, 42.70.Nq

I. INTRODUCTION

The development of artificially structured, composite materials (metamaterials) has substantially extended the range of possible electromagnetic (EM) responses that can be obtained by naturally occurring materials. The first demonstration of such a metamaterial at microwave frequencies showed negative refraction index in a narrow frequency band [1], in accordance with earlier theoretical predictions [2]. Negative index materials, which require simultaneously effectively negative dielectric permittivity ϵ_{eff} and magnetic permeability μ_{eff}, are also known as left-handed metamaterials (LHMs) [3]. Recent experiments demonstrated that the above requirement can be attained up to optical frequencies [4], which include the technologically relevant terahertz (THz) frequency regime. Most of the experimentally studied LHMs are made from periodic arrays of split-ring resonators (SRRs) and metallic wires.

Naturally, the theory of LHMs has been extended to account for nonlinear effects. A concise analytical framework for the nonlinear behavior of LHMs has been recently proposed, either by embedding the SRRs in a nonlinear dielectric [5,6], or by inserting certain nonlinear elements in each SRR slit [7,8]. Both ways lead to effectively field-dependent values of ϵ_{eff} and μ_{eff}. In addition, dynamical tuning of LHMs is achieved by inserting the nonlinear material in SRR slits [9]. The same effect is obtained through developing the metal structures of LHMs on nonlinear photorefractive crystals [10,11], as GaAs and $LiNbO_3$, which feature a saturable nonlinearity. Nonlinear effects are also apparent from the detection of second harmonic generation in SRR-based magnetic metamaterials on a glass substrate [12]. Moreover, the existence of nonlinear excitations such as discrete breathers and solitons in nonlinear metamaterials has been suggested [13–15]. In the present work we address the properties of LHMs with saturable nonlinearity.

II. EFFECTIVE PERMITTIVITY AND PERMEABILITY

We consider a two-dimensional (2D) metamaterial of circular SRRs with round cross section and long wires. The SRRs, with average radius a and cross-sectional diameter h, are arranged in a tetragonal lattice of constant d. The wires are located in the middle of the SRR rows, so that they form a lattice with period d. For simplicity we assume that they have only one slit of width d_g. Each SRR can be viewed as a small LC-oscillator circuit, where L and C are the SRR inductance and capacitance, respectively, having an inductive-capacitive resonance at a specific frequency $\omega_0 \simeq 1/\sqrt{LC}$. In the following we adopt the description (and notation) in Ref. [5], thus summarizing the essentials of the theory in a self-contained manner, omitting unnecessary details. Assuming that all metallic components are embedded in a nonlinear dielectric, the SRRs acquire a nonlinear capacitance C due to the dielectric filling their slits. Then, ϵ_{eff} is of the form

$$\epsilon_{eff} = \epsilon_D(|E|^2) - \omega_p^2/[\omega(\omega - i\gamma_\epsilon)], \tag{1}$$

where ω_p is the effective plasma frequency, γ_ϵ is the dielectric loss coefficient, ω is the frequency of the carrier wave, and $\epsilon_D(|E|^2)$ is the intensity-dependent part of the effective dielectric permittivity of the embedded dielectric [5].

In our study the photorefractive dielectric is embedded where the refractive index grating is generated via the electro-optic effect [16] (a second order χ^2 effect). The characteristic response time in the presence of the electro-optic effect and related phenomena allow us to consider the photorefractive material as "slowly" responding, which allows introduction of the slowly varying wave envelope approximation for modeling the propagation of low and medium intensity laser beams.

The $\epsilon_D(|E|^2)$ of the photorefractive dielectric is a nonlinear function of the electric field intensity whose nonlinear part can be of the saturable type [17]

$$\epsilon_D(|E|^2) = \epsilon_{D0} + \alpha \frac{|E|^2/E_c^2}{1 + \kappa|E|^2/E_c^2}, \tag{2}$$

where ϵ_{D0} is the linear dielectric permittivity, E_c is a characteristic electric field, $\alpha = +1$ (-1) for focusing (defocusing) nonlinearity, and κ is the saturation strength. That type of

nonlinearity has been employed extensively in discrete nonlinear Schrödinger equation models for the study of nonlinear excitations in photorefractive crystals [18–20]. Then, μ_{eff} can be written as

$$\mu_{eff}(|H|^2) = 1 + \frac{\hat{F}\omega^2}{\omega_{0nl}^2(|H|^2) - \omega^2 + i\Gamma\omega}, \tag{3}$$

where $\hat{F}=2\pi^2a^3/(c_0^2d^2L)$ is a filling factor (with c_0 being the light speed in vacuum), $|H|^2$ is the magnetic field intensity of the applied EM field, Γ is the magnetic loss coefficient, and $\omega_{0nl}(|H|^2)$ is the field-dependent resonant SRR frequency, due to the SRR field-dependent capacitance. The latter is given implicitly in terms of $|H|^2$ and ω by

$$\frac{|H|^2}{E_c^2} = A^2\frac{(1-X^2)[(\Omega^2-X^2)^2+\gamma^2\Omega^2]}{\Omega^2X^4[(\alpha+\kappa\epsilon_{D0})X^2-\kappa\epsilon_{D0}]} \tag{4}$$

where $A^2=\epsilon_{D0}^3h^2\omega_0^2/c_0^2$, and the following relations were used: $X=\omega_{0nl}/\omega_0$, $\Omega=\omega/\omega_0$, $\gamma=\Gamma/\omega_0$. Equation (4) reduces to the corresponding expression for the previously investigated cubic nonlinearity for $\kappa=0$ [5].

A. Phase diagrams

Equations (3) and (4) reveal that the magnetic (dimensionless) resonance frequency $X(|H|^2)$ is a multivalued function of $|H|^2$, leading to multiple possible magnetization states (MSs) for the metamaterial. The magnitude and the phase of those MSs with respect to the applied field can be such that the total magnetic response may be either positive or negative, which corresponds to either positive (right-handed property, RH) or negative μ_{eff} (left-handed property, LH), respectively. By varying the external field and/or its frequency, the metamaterial may switch between two different stable MSs, corresponding to different magnetic responses (positive or negative, with positive or negative μ_{eff}, respectively). For simplicity we comment on the case with neglected magnetic losses ($\gamma=0$), so that there are either one or three MSs.

In order to obtain global information for the multiplicity of the magnetic response and its sign as a function of the externally varied parameters $|H|^2$ and Ω we have constructed phase diagrams like those shown in Fig. 1. In Fig. 1(a) there is a region with one single negative response state (NRS) which, surprisingly, appears for $\Omega>1.2$ and its width increases with increasing $|H|^2$. It is remarkable that for the highest shown value of $|H|^2$ that region extends beyond $\Omega=1.4$. There are also large regions with single positive response states (PRSs), as well as smaller regions where three generally different magnetic response states coexist [see caption of Fig. 1(a)]. Similarly, in Fig. 1(b) is shown a region with one single NRS located around the linear resonance frequency ($\sim$1). Its width is slightly decreasing with increasing $|H|^2$. That region is surrounded by regions where a single PRS exists. There are also smaller regions where three generally different magnetic response states coexist. As an illustration, μ_{eff} is plotted as a function of $|H|^2$ for several values of Ω ($\alpha=-1$) in Fig. 2. The case with only one PRS is shown in Fig. 2(a), while the example of the passage from a region

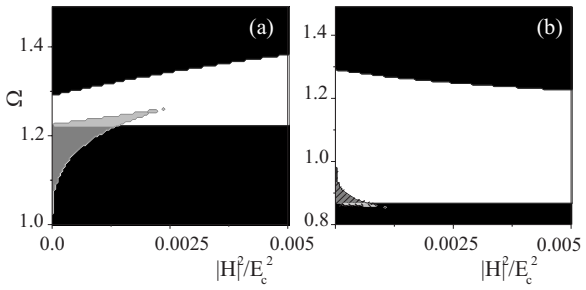

FIG. 1. Phase diagram in Ω-$|H|^2$ space showing the multiplicity of MSs in a metamaterial with saturable nonlinearity and the sign of the magnetic response: $A=0.32$, $\epsilon_{D0}=3$, $\hat{F}=0.4$, $\kappa=1$, and (a) $\alpha=-1$; (b) $\alpha=+1$. White: one negative MS; black: one positive MS; dark gray: one positive–two negative MSs; dark gray with pattern: one negative–two positive MSs; light gray: three negative MSs; light gray with pattern: three positive MSs.

with one PRS to one NRS is illustrated in Fig. 2(d). Generally in cases with a negative NRS, the metamaterial is the LHM proposing negative ϵ_{eff}.

The passage from a region with multiple states to another with only one state (or vice versa) occurs through bifurcations at specific parameter values of $|H|^2$ and Ω, as shown in Figs. 2(b) and 2(c). In Fig. 2(b) the system passes from a region of three possible MSs to a region with one MS with increasing $|H|^2$ ($\Omega=1.2$). In that specific case, the magnetic response of the metamaterial changes abruptly, with a jump from one branch of μ_{eff} to another at the bifurcation point which is located on a boundary in the corresponding phase diagram. Notice that here the multistability region is limited to rather low fields $|H|^2$. In Fig. 2(c) the metamaterial passes from a region of one MS with negative response to a region with three possible MSs, all of them with negative responses (LHM) which, however, differ in magnitude, with increasing $|H|^2$. In that case, the state of the system changes continu-

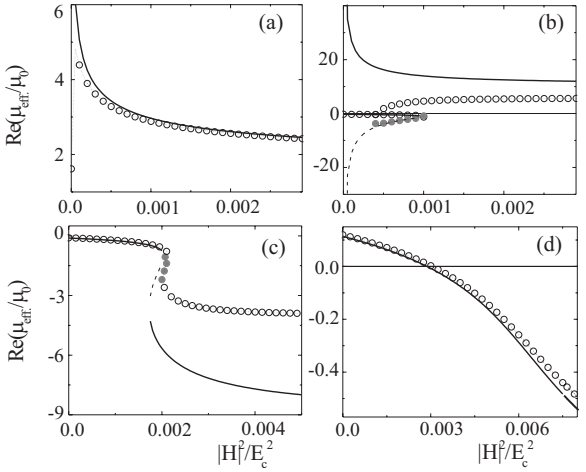

FIG. 2. Real part of μ_{eff} vs $|H|^2/E_c^2$ for a metamaterial with saturable nonlinearity, with $\alpha=-1$, $A=0.32$, $\epsilon_{D0}=3$, $\hat{F}=0.4$, $\kappa=1$, and (a) $\Omega=1.01$; (b) $\Omega=1.2$; (c) $\Omega=1.25$; (d) $\Omega=1.35$. The solid and dashed curves (or empty and filled circles) depict stable and unstable states of the SRR system [5] for $\gamma=0$ (or $\gamma=0.05$), respectively.

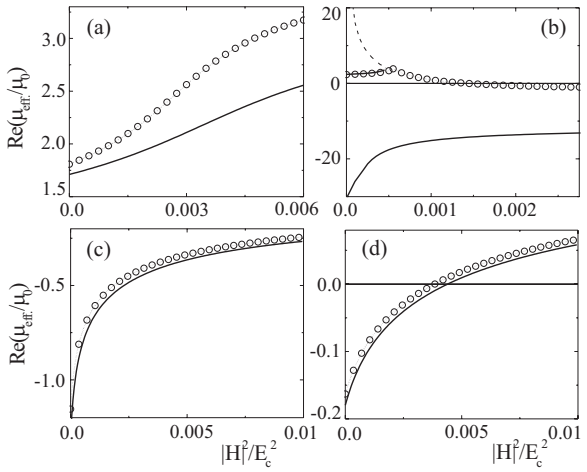

FIG. 3. The same as in Fig. 2 for $\alpha=+1$, $A=0.32$, $\epsilon_{D0}=3$, $\hat{F}=0.4$, $\kappa=1$, and (a) $\Omega=0.8$; (b) $\Omega=0.88$; (c) $\Omega=1.1$; (d) $\Omega=1.23$.

ously, when crossing the boundary to enter into the multistability region. Similar remarks also hold for Fig. 3, where μ_{eff} as a function of $|H|^2$ is plotted for several values of Ω and focusing nonlinearity ($\alpha=+1$).

The real and imaginary parts of the effective magnetic permeability versus the magnetic field intensity in the presence of the structure losses are illustrated in Figs. 2–5. In general, both of them behave according to Ref. [5]. It is worthwhile to stress two points. The first one is that the structure losses are the most effective in the field region with multiple μ_{eff} roots (in the case $\gamma=0$). There is an indication that in increasing γ the multiplicity regions shrink [Figs. 2(b) and 3(b)] which may lead to the shrinking of the regions with the left-handed properties. The second point is the possibility of controlling the imaginary part of μ_{eff} which determines the losses by a proper choice of the intensity of the external magnetic field (Figs. 4 and 5). These two features may be important for the future applications of left-handed materials.

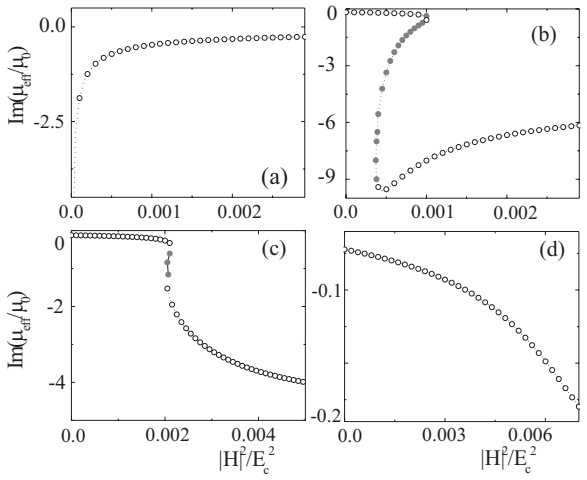

FIG. 4. Imaginary part of μ_{eff} vs $|H|^2/E_c^2$ for a metamaterial with saturable nonlinearity, with $\alpha=-1$, $A=0.32$, $\epsilon_{D0}=3$, $\hat{F}=0.4$, $\kappa=1$, and (a) $\Omega=1.01$; (b) $\Omega=1.2$; (c) $\Omega=1.25$; (d) $\Omega=1.35$. The curves with empty and filled circles depict stable and unstable states of the SRR system [5] for $\gamma=0.05$, respectively.

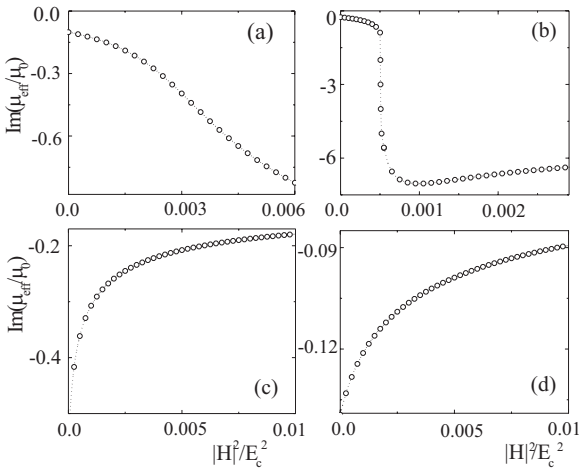

FIG. 5. The same as in Fig. 4 for $\alpha=+1$, $A=0.32$, $\epsilon_{D0}=3$, $\hat{F}=0.4$, $\kappa=1$, and (a) $\Omega=0.8$; (b) $\Omega=0.88$; (c) $\Omega=1.1$; (d) $\Omega=1.23$.

B. Cubic vs saturable nonlinearities

Comparison between the phase diagrams for metamaterial with the same parameters but different forms of nonlinearity reveals in some cases distinct differences. A typical example of a self-defocusing structure is illustrated for cubic [Fig. 6(a)] and saturable [Fig. 6(b)] nonlinearities. There are obvious differences, especially for high fields, where for the saturable metamaterial the region of a single NRS seems to become wider with increasing field. The corresponding LH region for the cubic metamaterial is missing. As noted above, the negative response in the case with saturable nonlinearity appears at rather high frequencies with respect to the linear magnetic resonance. In each of Figs. 6(a) and 6(b) there are also smaller regions at low fields, where multiple magnetic response states exist. The most important are the regions with two PRSs–one NRS and two NRS –one PRS in Fig 6(a), as well as the regions with three NRSs and two NRSs–

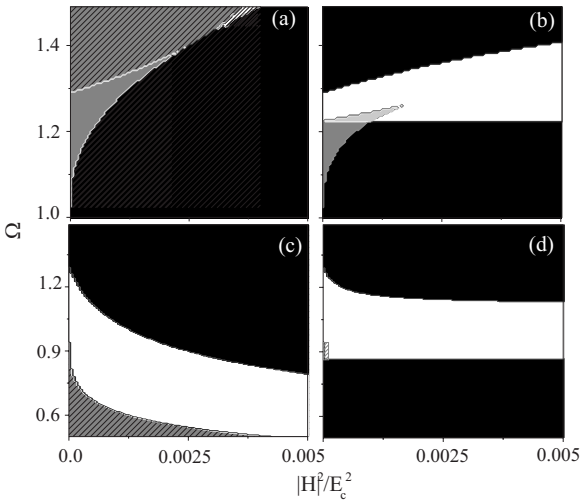

FIG. 6. Phase diagrams for $A=0.27$, $\alpha=-1$, (a) cubic and (b) saturable nonlinearity; $A=0.065$, $\alpha=+1$, (c) cubic and (d) saturable nonlinearity. Other parameters are $\epsilon_{D0}=3$, $\hat{F}=0.4$. Meaning of different areas is the same as in Fig. 1.

one PRS in Fig 6(b). Another typical example for a self-focusing metamaterial for both nonlinearities is shown in Figs. 6(c) and 6(d). For saturable nonlinearity [Fig. 6(d)], the region of one NRS is located around the linear resonance exhibiting rather large width, which is approximately constant and within the same frequency band for high fields. In contrast, for cubic nonlinearity [Fig. 6(c)], the region of one NRS, while it retains its width with increasing field, moves gradually to lower frequency bands well below the linear resonance. In this case there are also other qualitative differences, with the most important being the large multistability region at the lower-left corner of Fig. 6(c), which is absent in Fig. 6(d).

III. STABILITY

To assess the stability of the various magnetic response states, i.e., to clarify whether they are capable of supporting EM wave propagation in the metamaterial, we need to perform rigorous stability analysis. As a rule, the stability analysis of the SRR structure [5] shows in cases with one MS the stability of the only MS. In the multistability regions, with three generally different MSs, only two of them are simultaneously stable, leading to magnetization loops with varying fields.

The propagation of EM waves in the media under consideration is governed by Maxwell's laws. However, with respect to the characteristics of the photorefractive media (Sec. II A) the nonlinear modulation of propagating wave amplitudes can be described by two coupled nonlinear Schrödinger (NLS) equations, as is already shown for cubic nonlinearity [21]. For saturable dielectric nonlinearity, the complicated field dependence of μ_{eff} in Eq. (3) can be described by an expression of the form

$$\mu_{eff} = \mu + \mu_{NL}, \quad \mu_{NL} = \beta \frac{|H|^2/E_c^2}{1+\lambda|H|^2/E_c^2}, \tag{5}$$

where μ and μ_{NL} are the linear and nonlinear parts of μ_{eff}, respectively. The parameter μ and the coefficients β, λ can be obtained in each specific case by fitting numerically the exact μ_{NL} to Eq. (5). The last equation is appropriate for fitting the μ_{eff} resulting from both saturable and cubic dielectric nonlinearity, up to very high fields, while the fitting with modified Eq. (5) with cubic magnetic nonlinearity is limited to very low fields. A typical example is shown in Fig. 7, where μ_{eff} fits fairly well with the saturable expression for magnetic nonlinearity given by Eq. (5). Assuming that ϵ_{eff} and μ_{eff}, given by Eqs. (1), (2), and (5), respectively, are of second order, we can obtain by reductive perturbation of the corresponding Maxwell's equations [21] a pair of coupled saturable NLS equations for the propagation of EM waves in a saturable medium

$$i\frac{\partial \mathcal{E}}{\partial T} + P\frac{\partial^2 \mathcal{E}}{\partial X^2} + Q_1 \frac{|\mathcal{E}|^2 \mathcal{E}}{1+\kappa|\mathcal{E}|^2} + Q_2 \frac{|\mathcal{H}|^2 \mathcal{E}}{1+\lambda|\mathcal{H}|^2} = 0, \tag{6}$$

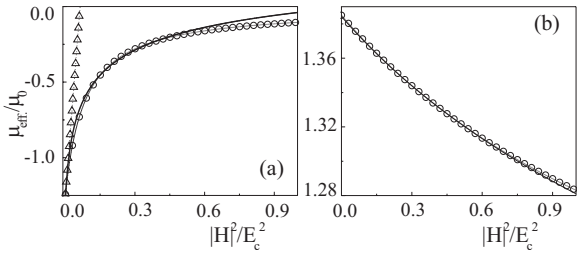

FIG. 7. Fitting of the numerically obtained μ_{eff} (solid curves) with the expression (5) (circles), for $A=3$, $\epsilon_{D0}=3$, $\hat{F}=0.4$, and cubic dielectric nonlinearity: (a) $\alpha=+1$, $\Omega=1.1$; (b) $\alpha=-1$, $\Omega=0.7$. Triangles correspond to a fitting to an expression for μ_{eff} with cubic nonlinearity.

$$i\frac{\partial \mathcal{H}}{\partial T} + P\frac{\partial^2 \mathcal{H}}{\partial X^2} + Q_1 \frac{|\mathcal{E}|^2 \mathcal{H}}{1+\kappa|\mathcal{E}|^2} + Q_2 \frac{|\mathcal{H}|^2 \mathcal{H}}{1+\lambda|\mathcal{H}|^2} = 0, \tag{7}$$

where $\mathcal{E}$, $\mathcal{H}$ are the slowly varying field amplitudes normalized to E_c, $P=\omega''(k)/2=(c^2-\omega^2)/(2\omega)$ $(P>0)$, $Q_1=\omega c^2\alpha\mu/(2c_0^2)$, and $Q_2=\omega c^2\beta\epsilon/(2c_0^2)$, with $c=c_0/\sqrt{\mu\epsilon}$ being the light speed in the medium. Equations (6) and (7) support monochromatic envelope wave solutions of the form $\{\mathcal{E}(X,T),\mathcal{H}(X,T)\}=\{\mathcal{E}_0,\mathcal{H}_0\}\exp(i\Omega_e T)$, where $\Omega_e \equiv (Q_1|\mathcal{E}_0|^2/(1+\kappa|\mathcal{E}_0|^2)+Q_2|\mathcal{H}_0|^2/(1+\lambda|\mathcal{H}_0|^2))$ is the (slow) frequency of modulated field envelopes, $\mathcal{E}_0,\mathcal{H}_0=$const, and X and T are the slow spatial and temporal variables, respectively. Here it is worth noting that in Ref. [22] the ultrashort pulse propagation in nonlinear left-handed media is described by the generalized nonlinear Schrödinger equation which was derived from the first principles. However, the photorefractive materials are slow responding [16] and characterized by the saturable nonlinearity which allows mathematical modeling in a slow envelope approximation [17].

In order to study the stability of the above monochromatic wave solution, we set $\mathcal{E}_0 \to \mathcal{E}_0 + \xi\mathcal{E}_1(X,T)$, $\mathcal{H}_0 \to \mathcal{H}_0 + \xi\mathcal{H}_1(X,T)$, where $\xi \ll 1$ and the perturbations $\mathcal{E}_1$ and $\mathcal{H}_1$ are complex functions of $\{X,T\}$. From this point we follow the procedure of Ref. [23], and generalize the results for saturable nonlinearity. Specifically, if the following criterion is met:

$$\tilde{k}^2 - \frac{\omega c_0^2}{c^2 P}\left(\frac{\alpha\mu\mathcal{E}_0^2}{(1+\kappa\mathcal{E}_0^2)^2} + \frac{\beta\epsilon\mathcal{H}_0^2}{(1+\lambda\mathcal{H}_0^2)^2}\right) \equiv \tilde{k}^2 - \frac{\omega c_0^2}{c^2 P}K' > 0, \tag{8}$$

where $\tilde{k}$ and $\tilde{\omega}$ are the perturbation wave number and frequency, respectively, then the propagating EM wave will be modulationally stable. Since $P>0$, the EM stability profile will essentially depend on K'. For LHMs, for which $\epsilon_{eff}, \mu_{eff} < 0$, the stability of a wave on a specific MS branch generally depends both on α, β and the field amplitude and frequency. More specifically, for the curves shown in Figs. 2 and 3, for α and β positive (negative) then the EM wave is stable (unstable), while for α and β having different signs the stability of the EM wave depends in each case on the value of $|H|^2$.

IV. CONCLUSIONS

We considered a 2D SRR-based LHM with saturable photorefractive nonlinearity. The form of nonlinearity, i.e., saturable versus cubic, can introduce significant quantitative differences between the two cases. The negative response in the case with saturable nonlinearity appears at rather high frequencies with respect to the linear magnetic resonance. This may be of technological importance, since recent efforts in designing LHMs aim to increase their operating frequencies to the THz frequency range with increasing their magnetic resonance frequency. Thus, it seems possible to increase the operating frequency of LHMs (i.e., the frequency band where the magnetic response and thus μ is negative) by purely nonlinear mechanisms. It is also shown that the magnetic response with saturable nonlinearity fits fairly well for both the cubic and saturable dielectric nonlinearities, up to very high fields. Finally, here it is indicated that the structure losses may act out in favor of the left-handedness.

ACKNOWLEDGMENTS

A.M. and L.H. acknowledge the support of the Ministry of Science, Serbia (Project No. 141034). G.P.T. and N.L. acknowledge support from the grant "PYTHAGORAS II" (KA. 2102/TDY 25) of the Greek Ministry of Education and the European Union. N.L. gratefully acknowledges the members of the Vinča Institute in Belgrade for supporting his visit.

[1] R. Shelby *et al.*, Science **292**, 77 (2001).
[2] V. G. Veselago, Sov. Phys. Usp. **10**, 509 (1968)[Sov. Phys. Usp. **92**, 512 (1967)].
[3] J. B. Pendry, Contemp. Phys. **45**, 191 (2004); S. A. Ramakrishna, Rep. Prog. Phys. **68**, 449 (2005).
[4] C. M. Soukoulis *et al.*, Science **315**, 47 (2007); V. M. Shalaev, Nat. Photonics **1**, 41 (2007).
[5] A. A. Zharov, I. V. Shadrivov, and Y. S. Kivshar, Phys. Rev. Lett. **91**, 037401 (2003).
[6] S. O'Brien, D. McPeake, S. A. Ramakrishna, and J. B. Pendry, Phys. Rev. B **69**, 241101(R) (2004).
[7] M. Lapine, M. Gorkunov, and K. H. Ringhofer, Phys. Rev. E **67**, 065601(R) (2003).
[8] J. B. Pendry *et al.*, IEEE Trans. Microwave Theory Tech. **47**, 2075 (1999).
[9] A. Derigon, J. J. Mock, and D. R. Smith, Opt. Express **15**, 1115 (2007).
[10] W. J. Padilla, A. J. Taylor, C. Highstrete, M. Lee, and R. D. Averitt, Phys. Rev. Lett. **96**, 107401 (2006).
[11] C. Helgert, C. Rochstuhl, T. Pertsch, E. -B. Kley, and A. Tünnermann, in *IEEE CLEO Europe—IQEC* (Fraunhofer Publica, Munich, 2007).
[12] M. W. Klein *et al.*, Science **313**, 502 (2006).
[13] N. Lazarides, M. Eleftheriou, and G. P. Tsironis, Phys. Rev. Lett. **97**, 157406 (2006).
[14] Y. Liu, G. Bartal, D. A. Genov, and X. Zhang, Phys. Rev. Lett. **99**, 153901 (2007).
[15] S. Bian, J. Frejlich, and K. H. Ringhofer, Phys. Rev. Lett. **78**, 4035 (1997).
[16] G. A. Brost, R. A. Motes, and J. R. Rotge, J. Opt. Soc. Am. B **5**, 1879 (1988); D. N. Christodoulides and M. I. Carvalho, *ibid.* **13**, 1628 (1996).
[17] V. O. Vinetskii and N. V. Kukhtarev, Sov. Phys. Solid State **16**, 2414 (1975) [Sov. Phys. Solid State **16**, 3714 (1975)].
[18] Lj. Hadžievski, A. Maluckov, M. Stepić, and D. Kip, Phys. Rev. Lett. **93**, 033901 (2004).
[19] M. Stepić, D. Kip, Lj. Hadžievski, and A. Maluckov, Phys. Rev. E **69**, 066618 (2004).
[20] A. Maluckov, M. Stepić, D. Kip, and Lj. Hadžievski, Eur. Phys. J. B **45**, 539 (2005).
[21] N. Lazarides and G. P. Tsironis, Phys. Rev. E **71**, 036614 (2005).
[22] M. Scalora, M. S. Syrchin, N. Akozbek, E. Y. Poliakov, G. D'Aguanno, N. Mattiucci, M. J. Bloemer, and A. M. Zheltikov, Phys. Rev. Lett. **95**, 013902 (2005).
[23] I. Kourakis and P. K. Shukla, Phys. Rev. E **72**, 016626 (2005).